NASA Technical Memorandum 83410

Spherical Micro-Glass Particle Impingement Studies of Thermoplastic Materials at Normal Incidence

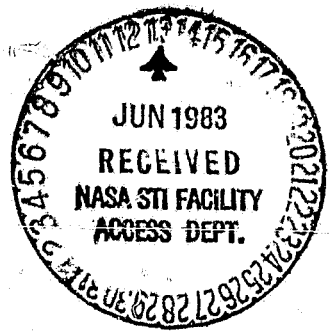

P. Veerabhadra Rao and Donald H. Buckley
Lewis Research Center
Cleveland, Ohio

Prepared for the
Joint Lubrication Conference
cosponsored by the American Society of Lubrication Engineers
and the American Society of Mechanical Engineers
Hartford, Connecticut, October 18–20, 1983

NASA

SPHERICAL MICRO-GLASS PARTICLE IMPINGEMENT STUDIES OF THERMOPLASTIC MATERIALS AT NORMAL INCIDENCE

P. Veerabhadra Rao[1] and Donald H. Buckley
National Aeronautics and Space Administration
Lewis Research Center
Cleveland, Ohio 44135

SYNOPSIS

Light optical and scanning electron microscope studies were conducted to characterize the erosion resistances of polymethyl methacrylate (PMMA), polycarbonate (PC), polytetrafluoroethylene (PTFE) and ultra-high-molecular-weight-polyethylene (UHMWPE). Erosion was caused by a jet of spherical micro-glass beads at normal impact. During the initial stages of damage, the surfaces of these materials were studied using a profilometer. Material buildup above the original surface was observed on PC and PMMA. As erosion progressed, this buildup disappeared as the pit became deeper. Little or no buildup was observed on PTFE and on UHMWPE. UHMWPE and PTFE are the most resistant materials and PMMA the least. Favorable properties for high erosion resistance seem to be high values of ultimate elongation, and strain energy and a low value of the modulus of elasticity. Erosion-rate-versus-time curves of PC and PTFE exhibit incubation, acceleration and steady state periods. A continuously increasing erosion rate period was observed however for PMMA instead of a steady state period. At early stages of damage and at low impact pressures material removal mechanisms appear to be similar to those for metallic materials. "Flake-like" debris was observed on the surface which is indicative of deformation wear by repeated impact and eventual fatigue,

E-1591

[1]NRC-NASA Research Associate.

causing material loss. At higher impact pressures evidence of melting of the surface was noted, which is believed to be the result of heat generated by impact.

INTRODUCTION

The damage and erosion caused by the impact of solid particles on the surfaces of aircraft engine components (1 to 5), helicopter blades (6), rocket motor nozzles (7), missiles (5), Earth satellites (8), and space vehicles (9) have received increased attention in recent years. In addition to metallic materials, plastic materials are being used in increasing amounts in structures as well as for viewing screens, windows, and metallic surface protection. This is mainly due to their high-strength, resilience and good fatigue resistance properties as well as low coefficient of friction and high resistance to abrasion. Some deleterious effects of erosion on nometallic surfaces are the loss of visibility, degradation of electromagnetic properties, and interference with communications as well as material damage and loss. Material degradation can occur during operation of tactical aircraft during severe weather (e.g., dust and sand storms). Solid impingement erosion is also of vital interest in defense applications such as in optically guided missiles, for laminated plastic transparent windshields, and canopies (10).

Some invesigators have concentrated on parametric studies and others on the erosion characteristics and resistance of polymeric, elastomeric, and plastic bulk materials (2, 3, 7, 11 to 19) and coatings (7, 18, and 20). Normal impingement studies of various plastic materials are briefly mentioned in this paper. Thus, epoxy resin (2 and 15), nylon (2, 14, 15, and 17), polypropylene (3, 14, 15), Tufnol (7), perspex (7, 13), and polyurethane (15) have been studied. On the other hand, polyurethane, polyvinylidene fluoride,

and fluorocarbon (14, 18, and 20) coatings have been examined to investigate their resistance during solid particle impingement. Solid impingement erosion of bulk plastics materials has received little emphasis in the past (10) due to their limited applications as structures. However, in view of their widespread use as coatings for aircraft radomes, antenna covers, and external skin protection, there are many instances of damage and erosion in real situations (6, 20).

The objective of this paper is to present the erosion characteristics of four commonly known thermoplastic materials namely polymethyl methacrylate (PMMA), polycarbonate (PC), polytetrafluoroethylene (PTFE), and ultra-high-molecular-weight-polyethylene (UHMWPE) by a jet of spherical micro-glass beads at normal incidence. Spherical glass bead particles have been used primarily for two reasons. (1) Small coal ash particles were observed to be spherical in shape, and (2) spherical particles cause a deformation type wear mechanism observed in several wear processes in real situations. Erosion mechanisms and the effect of time on erosion are discussed,based on optical light photographs, scanning electron micrographs and surface traces. These materials have been considered primarily because of their good tribological and abrasion resistance (PTFE AND UHMWPE), high strength and impact resistance (PC), and good optical transmittance and shatter resistant properties (PMMA) (21). This paper is in part a condensed version of reference (22).

MATERIALS

Specimen materials were PMMA, PC, PTFE and UHMWPE. The mechanical and other properties of these four thermoplastic materials are available in (22, 23). The specimens, which were 25 mm wide, 37 mm long, and 6.4 mm thick, were cleaned with alcohol and dried with compressed air.

APPARATUS AND EXPERIMENTAL PROCEDURE

The investigations in this paper were conducted with a commerical sand-blasting facility. Test specimens of plastic materials were eroded by normal incidence of commerical grade number 9 spherical glass bead particles (average diameter, ~ 20 μm; standard deviation, 12 μm). The glass bead particle distribution is presented in (22). Table I presents the properties of glass beads used in this study.

A schematic diagram of the steady-jet-impingement nozzle arrangement is shown in Fig. 1. The distance between the specimen and the nozzle (1.18 mm diam) was 13 mm. Argon was used as the driving gas at a 0.27 MPa (gage) pressure. The average particle velocity was 72 m/sec. The velocities were calculated by using a double disk arrangement similar to the one described by Ruff and Ives (24). The glass bead flow rate was 0.98 g/sec.

Before exposure all specimens were cleaned with distilled water and alcohol. The materials were tested in the as-received condition. The original surface roughness was 0.53 μm CLA for the PMMA and PC and 2.06 μm CLA for PTFE and UHMWPE. Specimens were weighed before and after each exposure to the impinging jet of glass beads, and weight loss values were converted to volume loss by dividing by density. Traces of the eroded surfaces were recorded with a profilometer, and the eroded surfaces were observed and photographed with optical light and scanning electron microscopes. The specimens that were prepared for SEM examination were gold sputter-coated, which is a commonly used technique.

RESULTS AND DISCUSSION

Erosion Progress and Morphology

The effects of glass bead impingement on PMMA and PC during the initial phases of erosion (from 3 to 60 sec) is shown in Figs. 2 and 3, respectively.

Separate specimens were tested for each exposure time shown in these figures in order to eliminate the effects of interrupted tests. The apparent reduction in the damage area with respect to exposure time, as observed in some cases in Figs. 2 and 3, are artifacts due to difficulties in focussing all areas of the pit with an optical microscope. Surface profiles at selected erosion intervals for these materials are shown in Figs. 4 to 6.

The damage patterns may be divided into four regions (indicated in Figs. 4 and 5). Region 1 is a central irregular pit surrounded by region 2, a nonuniform buildup of plastic material and glass. Region 2 consists of peaks and valleys from 30 to 100 μm deep. Region 3 is a slightly raised region which slopes toward the original surface. Region 4 is a depressed area 5 to 10 μm below the original surface level.

Evidence for material buildup can be seen in the surface traces of PMMA and PC (Figs. 4 and 5). These are believed to be due to heat distorsion or partial melting and redeposition of material during impingement. A temperature rise as high as 190° C during impact conditions has been reported (7). Also, increased levels of the glass bead material are observed in this area. Material buildup was negligible for PTFE (22) and UHMWPE. However, the surfaces of the PTFE specimens were observed to have changed color (from white to light brown) after glass bead impact. This color change is also believed to be due to the heat generated during impingement. It is reasonable that PTFE would be most affected by heat in view of its lower heat distortion temperature. Darkening of nylon and polypropylene surfaces due to solid impingement (14) has been attributed to a chemical change in the surface associated with localized heating. Figure 7 shows SEM micrographs of an eroded PMMA specimen exposed to glass bead impingement for 15 seconds (the same as the surface profile in Fig. 4(c)). These micrographs indicate

material buildup, a fissure between regions 2 and 3 (Fig. 7(a)), and layers or bands in some areas (Fig. 7(b)). These bands are, in general, circumferential arcs surrounding the center of impact with decreasing elevations away from the center of impact. They are believed to be formed by melting and resolidification of the plastic material. However, further studies are necessary to identify the mechanism(s) involved with the formation of these stratified layers.

As erosion progresses for PMMA, the pit in region 1 deepens and broadens (Figs. 2 and 4). Region 3 gradually deepens and disappears. After a 10-minute exposure all regions merge into the main pit. For PC, regions 3 and 4 are clear at first but gradually disappear with very long exposure (Fig. 5). In both cases, at advanced stages of erosion, the pit slopes (region 1) become very smooth. Figure 8 shows SEM micrographs of eroded specimens of PMMA, PC, and PTFE after 10-minute exposures.

Deep holes are observed for PMMA and PC. PTFE appears to retain a relatively unstructured damage pattern after 10 minutes (Fig. 8(c)). However, after a 15-minute exposure a layered structure is observed along the pit sides.

Erosion-versus-Time Curves

Cumulative erosion-versus-time curves for PMMA, PC, and PTFE are shown in Fig. 9. Table II presents the data for the four plastics at 5-, 10-, 15-, and 20-minute exposures. PMMA erodes rapidly compared with PC, PTFE and UHMWPE (also evident from surface profiles). UHMWPE followed by PTFE are observed to be the most resistant of the four plastic materials. The results in table II and Fig. 9 show good reproducibility for the erosion process of thermoplastic materials under normal impingement. The scatter of data increased with increasing volume loss.

Typical erosion volume loss-versus-time curves can be divided into different stages. The incubation or induction period exists when there is little or no weight loss. The acceleration period is the time during which the weight loss rate increases rapidly until it reaches a peak. After this there is often a constant or steady-state period, but in these experiments erosion rates increase for PMMA. Analysis of the data (11, 14-17) indicates that erosion rate versus time curves on nylon, plexidur, PMMA, polyproplyene and polyurethane exhibit incubation (and deposition), acceleration, and steady-state periods. Plots of carbon and glass reinforced nylon, however, show incubation, acceleration, peak erosion rate, and deceleration periods. The deceleration period is the time during which the weight loss rate decreases from a peak value. The effect of exposure time on erosion rate has been studied recently by the present authors (25). These types of curves have also been noticed on ductile metallic materials exposed to glass beads as well as angular particles.

Least squares fit straight lines through the average volume loss data were fitted and linear equations are included in table II to show the approximate slopes and intercepts for each material. The values of the slopes of the lines in mm^3/min can be used for comparative purposes: UHMWPE, 0.20; PMMA, 3.02; PC, 0.40; and PTFE, 0.23 mm^3/min.

Erosion Resistance

The erosion resistance varies directly with the ultimate elongation, strain energy, and maximum service temperature; it varies inversely with tensile strength, yield strength, and modulus of elasticity (22). No single property is clearly dominant in its effect on erosion resistance. It is believed, however, that some combination of high ultimate elongation, impact strength, maximum service temperature, and low modulus of elasticity all contribute to high erosion resistance.

A summary of erosion results and conditions on elastomeric and plastic materials tested by different investigators (2, 3, 7, 12 to 15) is presented in Ref. 22. It was observed that bulk composite materials, nylon, epoxy, and polypropylene to be less resistant to erosion than the metals tested. When PMMA was tested by other investigators (12, 13, 16, 19) using entirely different shapes and sizes of abrasive particles and different experimental devices, very low resistance to erosion was indicated when compared to other nonmetallic materials (consistent with our results). For elastomers, these investigators found that filled rubber tire tread showed the highest resistance of all nonmetallic materials tested to erosive wear (12, 26). Other investigations (27) have shown that natural and synthetic rubbers exhibit good erosion resistance because of their low modulus of elasticity and that some correlation exists with ultimate resilience (defined as (tensile strength)^2/[2 (modulus of elasticity)]) and with density of materials (16). The ultimate resilience for the materials examined does not vary sufficiently to arrive at the same conclusion in the current study.

Material Removal Processes

To more thoroughly study features of the material removal process during exposure to glass bead impingement, high magnification SEM micrographs were taken of the eroded specimens (Fig. 10). Platelets or flakes were observed which looked similar to those observed on aluminum alloy (28) under identical impingement conditions. However, on the aluminum alloy flakes, random impact impressions were noticed which were not observed on the plastic material flakes.

Tilly (14) has also reported observations of flakes on nylon, fiberglass, and epoxy resin surfaces due to angular particle impingement. Flakes were also observed by Evans and Lancaster for sliding of polyphenylene oxide and

polyacetal in n-hexane and n-propanol against stainless steel (29); by Shen and Dumbleton for dry sliding of polyoxymethylene against stainless steel (30), and by Shallamach for abrasion of particles and pins against different types of filled and unfilled rubber (26, 31, 32). The flakes observed in the present investigation are believed to form due to repeated direct impact and deformation followed by shear and partial removal during outflow of particles. The extent of heat distortion and melting, which may play an important role in this process, is unknown at present.

It has also been observed from the literature that plastic materials such as polypropylene, nylon, PMMA, natural rubber, and Vulkallan B (2, 13, 14, 27) behave as either brittle or ductile materials depending on the angle of impingement (22). Maximum erosion rates have been observed at angles between 15° and 35°, and cutting wear is indicated by sharp faceted surfaces. For higher incidence angles (including normal), the damage patterns (including the observation of flakes) appear similar to those for ductile metals. This is indicative of the predominance of wear due to deformation as opposed to cutting.

In our studies cutting wear as discussed in Ref. 33 appears to be absent for all four plastic materials. This was expected as most of the spherical glass beads were not broken even after impact (28), and the material was worn due to deformation by repeated impact and eventual fatigue rather than by cutting of the surface.

For PTFE the flakes appear thinner than those for the other two materials (Fig. 10). Thin flakes were also reported for the more resistant nylon in (14), and large flat flakes were reported in (15) for heavily eroded epoxy resin. Hence, thinner flake formation may be related to higher erosion resistance.

CONCLUSIONS

1. Initially, a buildup of material composed of a combination of target materials and erodent particles was observed around the pit for PC and PMMA during the early stages of damage. After further exposure material buildup and any other features on the surface disappeared as the main pit developed.

2. UHMWPE was found to be the most resistant to erosion and PMMA the least resistant.

3. Erosion-rate-versus-time curves exhibited incubation, acceleration and steady-state periods for PC, PTFE and UHMWPE. A continuously increasing erosion rate was observed for PMMA.

4. A combination of high ultimate elongation, strain energy, maximum service temperature, and low modulus of elasticity are consistent with high erosion resistance.

5. SEM micrographs show flake-type debris in the eroding pits of the thermoplastic materials. Material loss is believed to be due primarily to the breakup and removal of these flakes. Smaller, thinner flake formation appears to correlate with higher erosion resistance.

References

1. Sage, W.; and Tilly, G. P., "The significance of particale size in sand erosion of small gas turbines," J. R. Aeronaut, Soc., 73, May 1969, pp.427-428
2. Tilly, G. P., "Sand erosion of metals and plastics: a brief review," Wear, 14, 1969, pp. 241-248.
3. Goodwin, J. E., Sage, W., and Tilly, g. P., "Study of erosion by Solid particles, Proc. Inst. Mech. Eng., 184, no. 15, Part 1, 1969-70, pp. 279-292.
4. Williams, J. H., Jr.; and Lau, E. K., "Solid particle erosion of graphite-epoxy composites," Wear, 29, Aug. 1974, pp. 219-230.
5. Schmitt, G. F., Jr., "Impact erosion-a serious environmental threat to aircraft and missiles," ASME Paper 75-ENAS-45, July 1975.
6. Hibbert, W. A., "Helicopter trials over sand and sea," J. R. Aeronaut, Soc., 69, no. 659, Nov. 1965, pp. 769-776.
7. Neilson, J. H.; and Gilchrist, A., "An experimental investigation into aspects of erosion in rocket motor tail nozzles," Wear, 11, 1968, pp. 123-143.
8. Hoening, S. A., "Meteoric dust erosion problem and its effect on the earth satellite," Aeronaut. Eng. Rev., 16, July 1957, pp. 37-40.
9. Tilly, G. P. "Erosion by impact of solid particles," Treatise on Materials Science and Technology, 13, D. Scott, ed., Academic Press, 1979, pp. 287-319.
10. Schmitt, G. F., Jr., "Liquid and solid particle impact erosion," Wear Control Handbook, M. B. Peterson and W. O. Winer, eds., American Society of Mechanical Engineers, 1980, pp. 231-282.

11. Behrendt, A., "Solid impact," Proc. 3rd. Int. Conf. on Rain Erosin, A. A. Fyall and R. B. King Eds., pp. 797-820 (1970).

12. Russel, A. S.; and Lewis, J. E., "Abrasive characteristics of alumina particles," Ind. Eng. Chem., 46, June 1954, pp. 1305-1310.

13. Neilson, J. H.; and Gilchrist, A., "Erosion by a Stream of Solid Particles." Wear, 11, 1968, pp. 111-112.

14. Tilly, G. P., "Erosion caused by airborne particles," Wear 14, 1969, pp. 63-79.

15. Tilly, G. P.; and Sage, W., "The interaction of particle and Material behaviour in erosion processes," Wear, 16, 1970, pp. 447-465.

16. Kayser, W., "Erosion by solid bodies," Proceedings of the Second Meersburg Conference on Rain Erosion and Allied Phenomena, vol. 2, A. A. Fyall and R. B. King, eds., Royal Aircraft Establishment, Farnborough, England, 1967, pp. 427-447.

17. Tilly, G. P.; and Sage, W., "A study of the behavior of particles and materials in erosion processes," ASME Paper No. 69-WA/Met-6, Nov. 1969.

18. Behrendt, A., "Sand Erosion of Dome and Window Materials," International Conferene on Rain Erosion and Associated Phenomena. Royal Aircraft Establishment, Farnborough, England, 1975, pp. 845-861.

19. Soderberg, S.; et al., "Erosion classification of materials using a centrifugal erosion tester," Tribol. Int., 14, Dec. 1981. pp. 333-343.

20. Zahavi, J.; and Schmitt, G. F., Jr., "Solid particle erosion of polymeric Coatings," Wear, 71, Sept. 1981, pp. 191-210.

21. Bolz, R. E., and Tuve, G. L., eds., CRC Handbook of tables for Applied Engineering Science, The Chemical Rubber Co. pp. 105 (1970).

22. Rao, P. Veerabhadra, Young, S. G., and Buckley, D. H., NASA TP-2161, 1983.

23. Jones, W. R., Jr., "Effect of γ irradiation on the friction and wear of ultrahigh molecular weight polyethylene," Wear, 70, pp. 77-92.

24. Ruff, A. W., and Ives, L. K., "Measurement of Solid Particle Velocity in Erosive Wear," Wear, 35, 1975, pp. 195-199.

25. Rao, P. Veerabhadra, and Buckley, D. H., NASA TP-2169, 1983.

26. Schallamach, A., "On the abrasion of rubber", Proc. Phys. Soc., london, Sect. B, 67, part 12, Dec. 1954, pp. 883-891.

27. Eyre, T. S., "Wear Characteristics of Metals, " Tribol, Int., 9, Oct. 1976, pp. 203-212.

28. Rao, P. Veerabhadra, Young, S. G., and Buckley, D. H., "Morphology of Ductile Metals Eroded by a Jet of Spherical particles Impinging at Normal Incidence, Wear, 85, 1983, pp. 223-237.

29. Evans. D. C., and Lancaster, J. K., "The wear of polymers," Treatise on materials Science and Technology, D. Scott, ed., vol. 13, Academic Press, 1979, pp. 85-139.

30. Shen, C.; and Dumbleton, J. H., "The Friction and Wear Behavior of Polyoxymethylene in connection with Joint Replacement," Wear, 38, 1976, pp. 291-303.

31. Schallamach, A., "Abrasion of rubber by a needle," Polym. Sci., 9. 1952, pp. 385-404.

32. Schallamach, A., "Friction and abrasion of rubber," Wear, 1, 1957/1958, pp. 384-417.

33. Rao, P. Veerabhadra; Young, S. G.; and Buckley, D. H., NASA TP 2139, 1983.

TABLE I. - AVERAGE PROPERTIES AND SILICA CONTENT OF GLASS-BEAD MATERIAL

Density	2.5×10^3 kg/m^3
Hardness (Moh's scale)	6.0
Modulus of elasticity	77.34 GPa
Silica content	68 percent
Iron content	0.0415 percent
Refractive index	1.50 to 1.55
Specific heat (40° to 800° C)	0.27 cal/g
Coefficient of expansion (20° C to 300° C)	$0.5(10^{-6})$

TABLE II - EXPERIMENTAL DATA SCATTER AND CURVE FIT EQUATIONS

Material	Time t, min.	Number of specimens tested	Average volume loss V, mm^3	Standard deviation of volume loss	Curve Fit Equation V = A + mt	
PMMA[a]	5	8	8.39	0.20	A	m
	10	6	18.89	1.09	-9.07	3.02
	15	4	33.69	1.92		
	20	2	53.80	[b]N/A		
PC	5	8	1.10	0.32		
	10	6	3.04	.22	-0.90	0.40
	15	4	5.19	.10		
	20	2	7.03	[b]N/A		
PTFE	5	8	1.37	0.10		
	10	6	2.83	.19	+0.36	0.23
	15	4	3.91	.12		
	20	2	4.85	[b]N/A		

[a]Since the observations indicate that the erosion wear rate of PMMA is not constant with time, a linear least squares-fit may not be a good choice for regression analysis. A parabolic model provides a better fit to the experimental data and has an erosion rate which varies with time. Two such possible least-squares fit parabolic models are:

$$V = 1.13t + 0.077t^2$$

and

$$V = 6.13 + 0.120t^2$$

Theoretically, the prediction given by the first equation is observed to be the better fit of the two, since it has the property that the volume of erosion is zero at zero time. In real situations, however, an incubation period exists as shown schematically in figure 9 and the second equation may be suggested for predictions. Both equations however estimate the erosion loss correctly. The calculated values of average volume loss V using both equations varied from actual values by 0.6 to 10 percent.

[b]Not applicable.

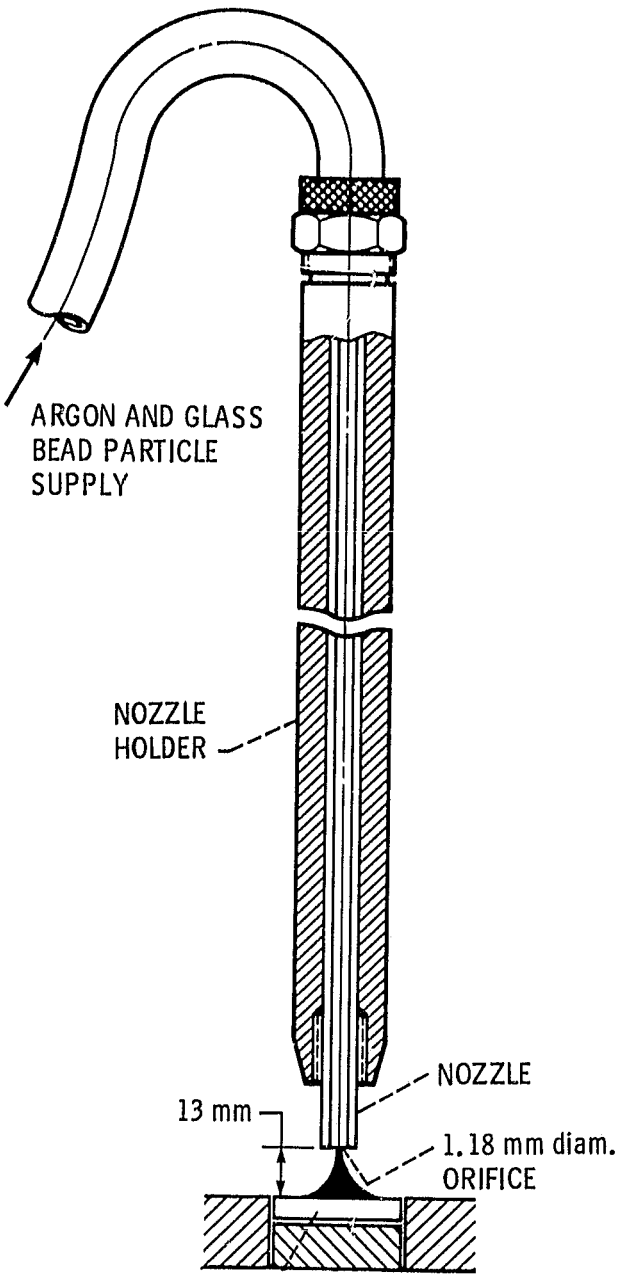

Figure 1. - Schematic diagram of nozzle holder arrangement for impingement apparatus at normal incidence.

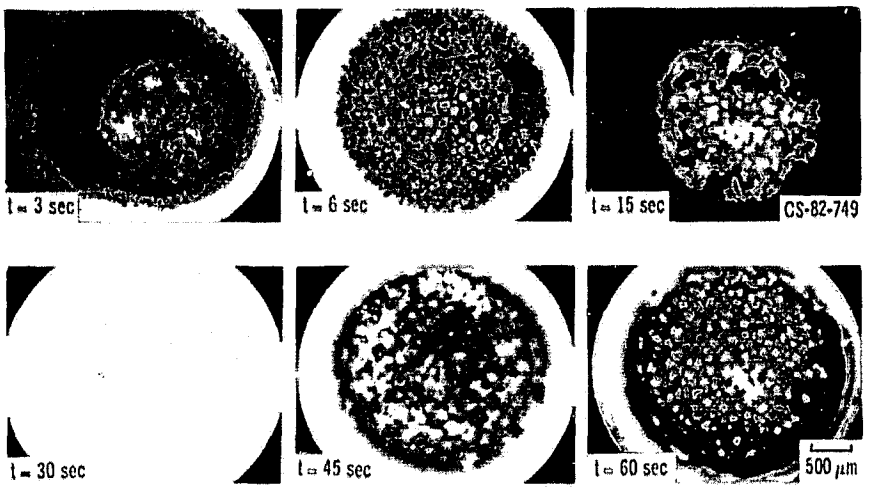

Figure 2. - Photomicrographs of polymethyl methacrylate (PMMA) surfaces during initial stages of glass bead impingement erosion. Gas pressure, 0.27 MPa. Particle velocity, 72 m/s.

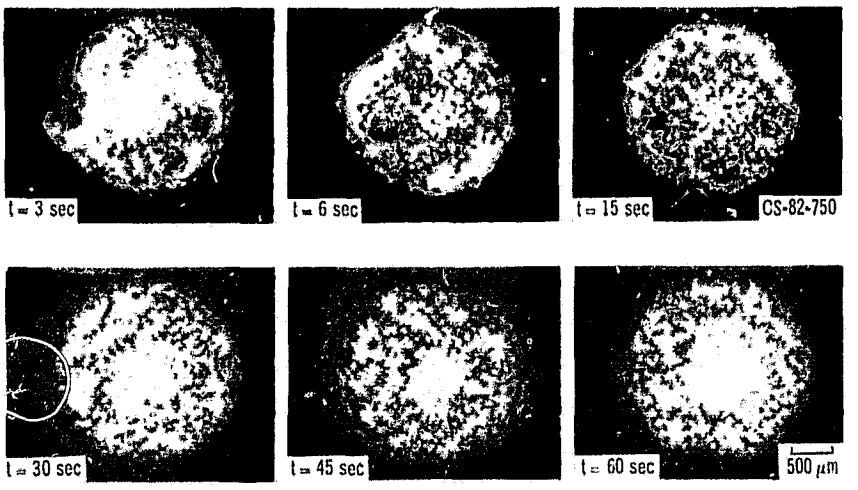

Figure 3. - Photomicrographs of polycarbonate (PC) surfaces during initial stages of glass bead impingement erosion. Gas pressure, 0.27 MPa. Particle velocity, 72 m/s.

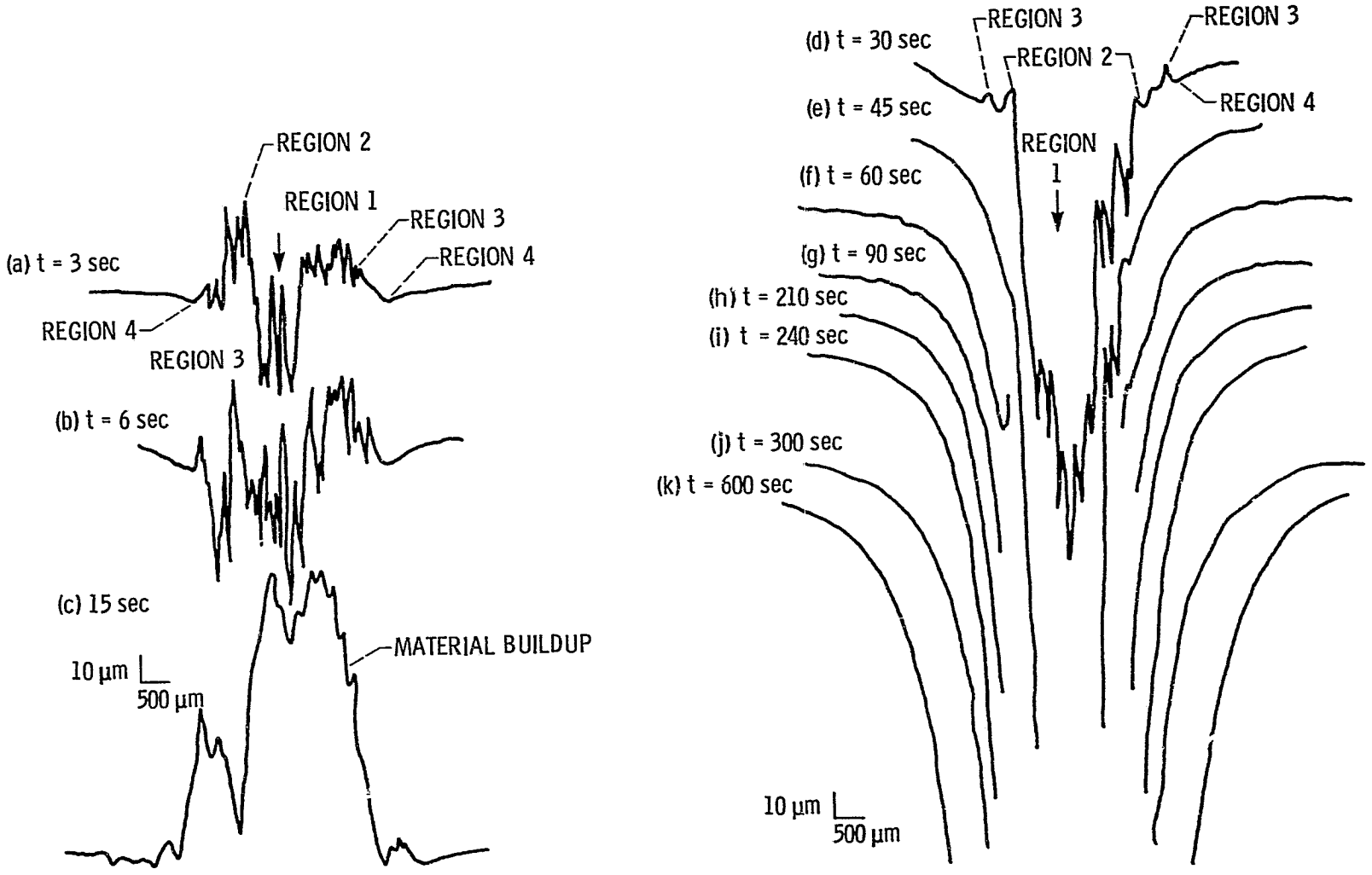

Figure 4. - Surface traces on PMMA as a function of time.

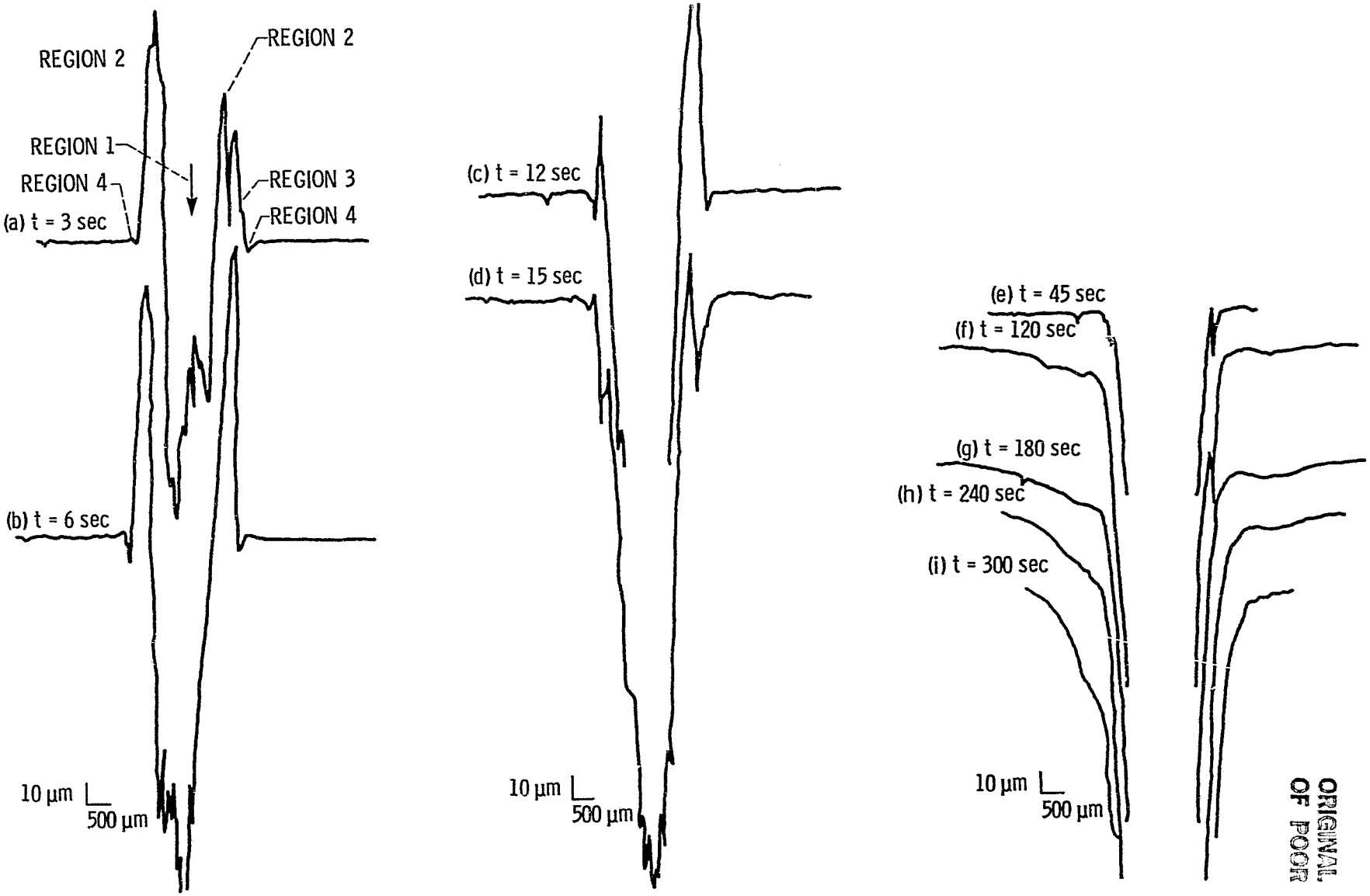

Figure 5. - Surface traces on polycarbonate as a function of time.

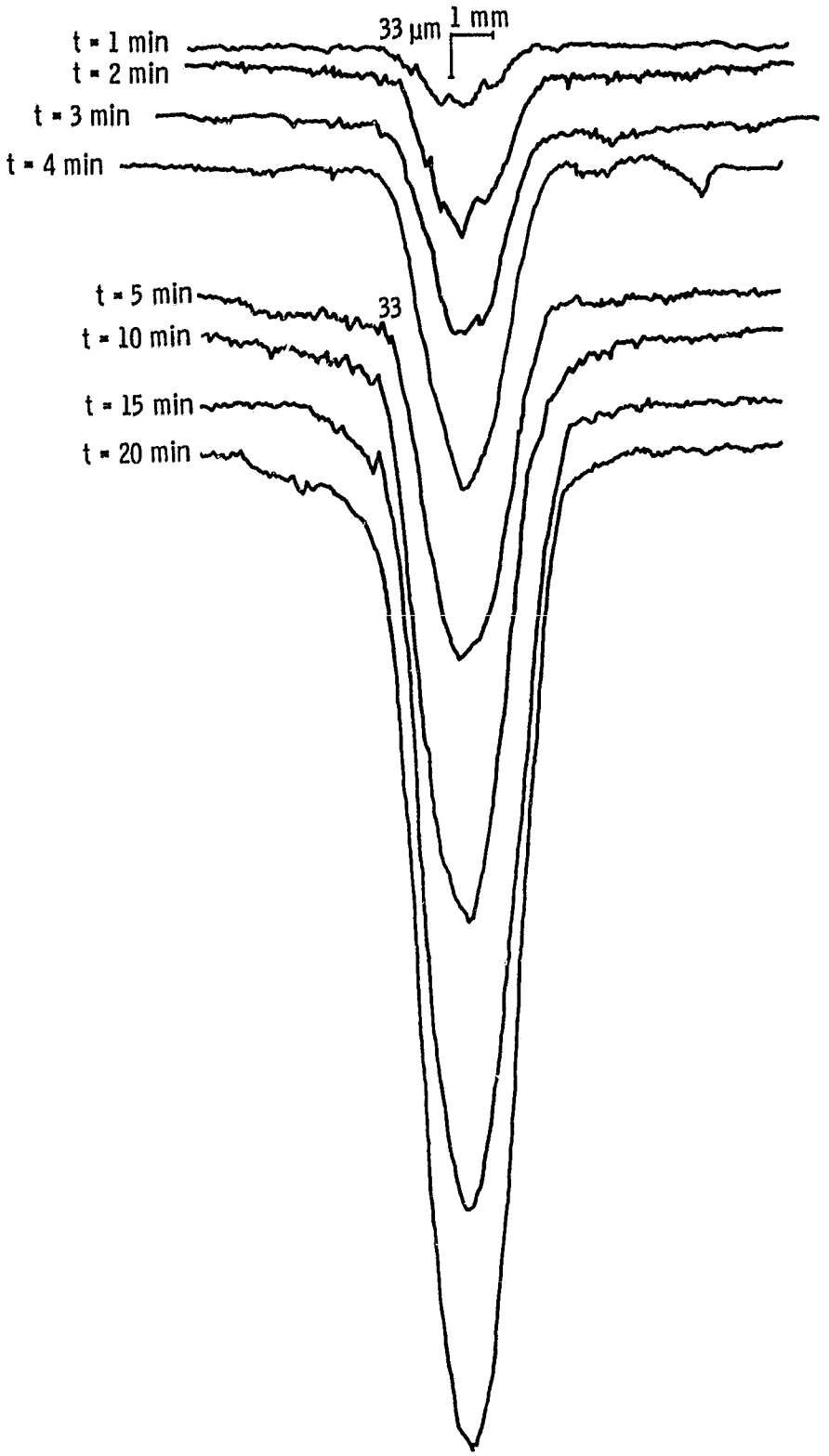

Figure 6. - Surface traces on PTFE as a function of time.

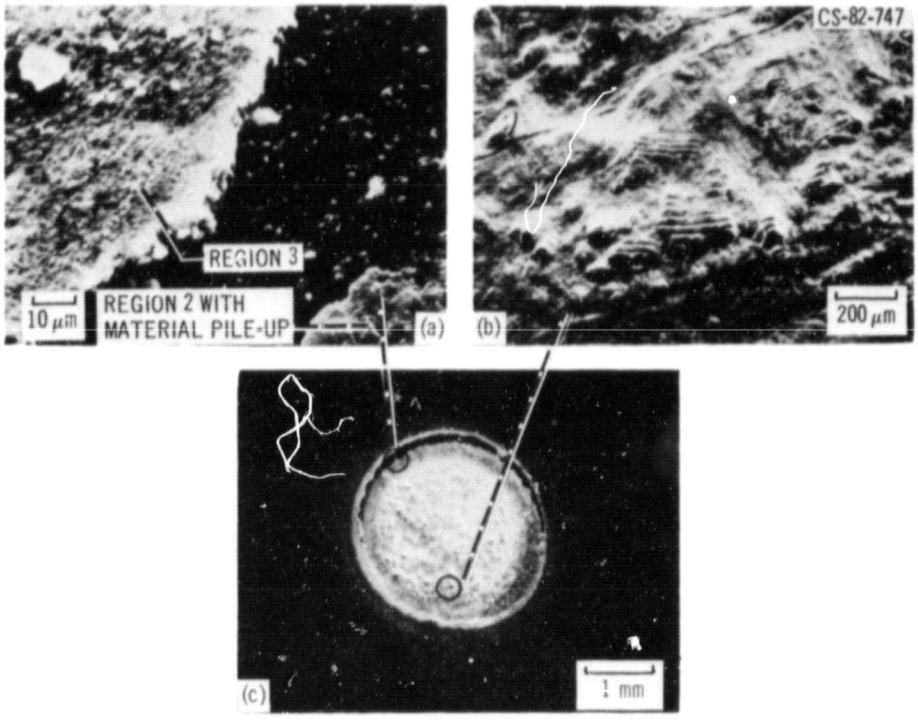

(a) Details of regions 2 and 3.

(b) Material buildup with possible stratification.

(c) Micrograph of material flow of an eroding pit.

Figure 7. - SEM micrographs (40° tilt) of PMMA specimen surface exposed to glass bead impingement. Time, 15 secs; gas pressure, 0.27 MPa. Particle velocity, 72 m/s.

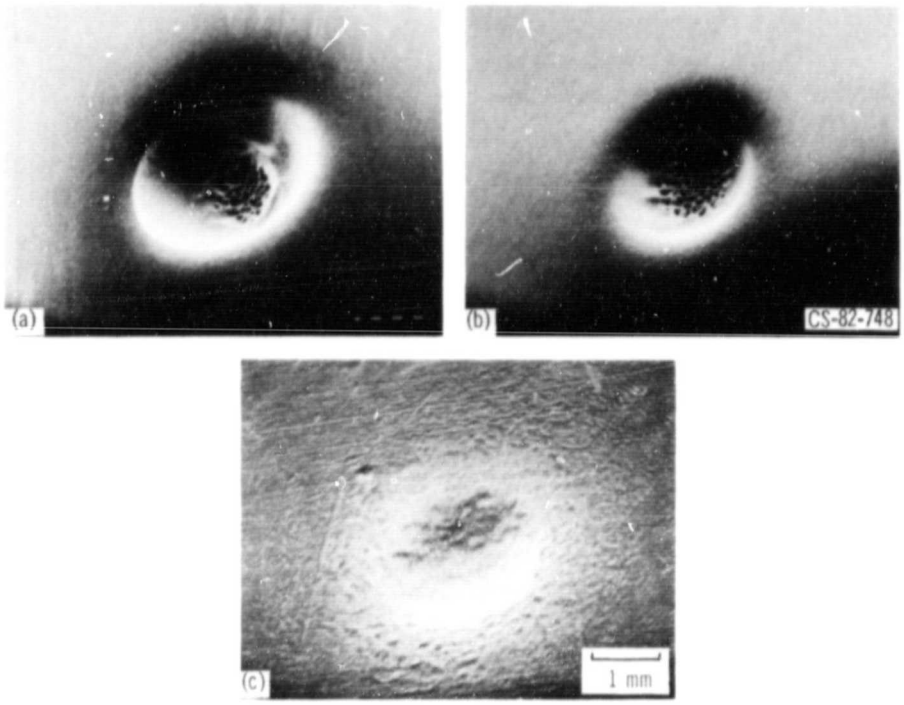

(a) PMMA

(b) Polycarbonate

(c) PTFE

Figure 8. - SEM micrographs (40° tilt) of eroded specimens exposed to glass bead impingement. Time, 10 min; gas pressure, 0.27 MPa. Particle velocity, 72 m/s.

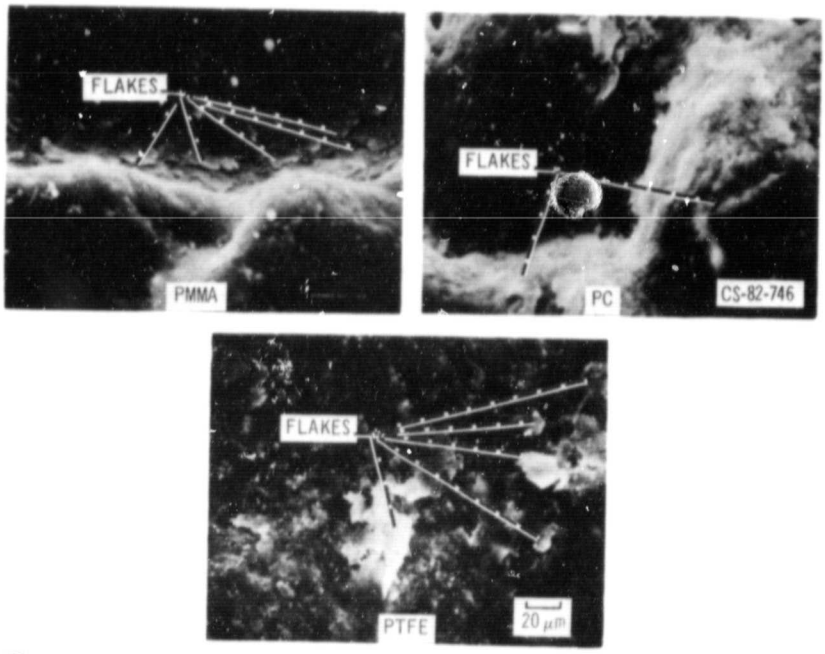

Figure 10. - SEM micrographs (40° tilt) of eroded thermoplastic material surfaces. Exposure time, 10 min; gas pressure, 0.27 MPa. Particle velocity, 72 m/s.